JOURNAL OF CATALYSIS 138, 500–517 (1992)

Preparation of Pd/SiO_2 Catalysts for Methanol Synthesis

III. Exposed Metal Fraction and Hydrogen Solubility

ADRIÁN L. BONIVARDI[1] AND MIGUEL A. BALTANÁS[2]

INTEC,[3] Güemes 3450, 3000—Sante Fe, Argentina

Received September 2, 1991; revised June 11, 1992

Tetramminepalladium complex was ion exchanged (IE) on purified, well characterized macro- and microporous Davison G-59 and G-03 silica gels (Pd loadings: 1.1–7.7% Pd w/w). These catalytic materials were reduced in hydrogen (473 to 723 K) after calcining them under both oxidating and inert atmospheres, in a wide range of experimental conditions. Two different regions were identified, each one showing its own dependence for the exposed metal fraction (FE) vs the maximum calcining temperature (T_c): (i) at $T_c < 423$ K the FE depends upon the Pd loading and also upon the type of Pd complex species remaining on the support right before initiating the H_2 reduction, whereas (ii) for $T_c > 423$ K the FE is a function of the metal loading and the support structure, but not of the complex species mentioned. Hydrogen solubility on these Pd/SiO_2 systems diminishes with the mean diameter of the metal crystallites, reaching a constant value for $\bar{d} < 20$ Å. The fraction of soluble hydrogen can be quantitatively decomposed into that of β-HPd and another one corresponding to hydrogen sorbed onto subsurface sites. It is shown that a suppression of H_2 solubility exists for the metal crystallites occluded by the microporous support.

INTRODUCTION

It is well documented that the activity and selectivity of supported Pd/SiO_2 catalysts toward the production of oxygenates depend upon the physico-chemical nature of their active components in a complex fashion. Even for a given choice of support and metal precursor the catalytic performance of this system is most often a strong function of the preparation method and/or the sequence of pretreatments prior to having an on-line process catalyst.

Thus, we set up an experimental program aimed at: (i) the controlled production of Pd/SiO_2 on a few, well-purified, characterized commercial macro- and microporous supports (Davison G-59 and G-03) with the systematic analysis of metal deposition, drying, calcination, and reduction steps; and (ii) their use for the activation of syngas at process conditions (T = 493–523 K; P = 1–4 MPa). A single preparation method, ion exchange (IE) of palladium acetate in aqueous ammonium hydroxide, was used, trying to exclude any possible promotional effects of chlorine or any other residual anion from the precursor on the catalyst performance and rather focusing the attention on the supports texture and the conditions of the IE themselves (*1*).

In part of that previous work, detailed analyses were made concerning the effects that thermal decomposition conditions have upon the final fate, or resulting product(s), of the precursor system $[Pd(NH_3)_4]^{2+}/SiO_2$ of these catalysts (*2*). Using both inert and oxidating atmospheres, two decomposition regions were identified. Two of the NH_3 ligands become lost in the first, low-temperature region (308–473 K), disregarding the type of decomposing atmosphere. In the second one (473–773 K), the final products

[1] Research Assistant from CONICET.

[2] Member of CONICET's Scientific and Technological Research Staff and Professor at UNL.

[3] Instituto de Desarrollo Tecnológico para la Industria Química. Universidad Nacional del Litoral (UNL) and Consejo Nacional de Investigaciones Científicas y Técnicas (CONICET).

0021-9517/92 $5.00

of the thermal decomposition of the amminepalladium complex onto the SiO_2 surfaces were found to be strongly dependent on the surrounding atmosphere and/or the support structure: Ultradispersed Pd^0 is the final product on both catalyst types when N_2 is the decomposing atmosphere, whereas either a mixture of $Pd^0 + [(SiO)_2]^{2-}Pd^{2+}$ (on the microporous G-03) or pure $[(SiO)_2]^{2-}Pd^{2+}$ (on the macroporous G-59) are the final products when air is employed.

Different authors have reported about the pronounced influence that the previous calcining conditions have on the reproducibility in obtaining a given fraction of total metal atoms exposed (FE) after the (final) reduction step of the catalyst preparation, most notably in the cases of $[Pt(NH_3)_4]^{2+}$/zeolite (*3–7*) and $[Pd(NH_3)_4]^{2+}$/zeolite (*4, 8–10*). These workers have concurred in reporting the existence of an optimal calcination temperature (T_c) in air for which maxima FEs are obtained, which seems to be characteristic of the supported metal involved (*3, 5, 7, 9*). The origin of this unique feature has been correlated with the presence of more or less remaining NH_3 ligands surrounding the metal cation prior to the reducing step (*3, 9*).

Since this paper deals with the production of materials, Pd/SiO_2, apt for manufacturing methanol with high selectivity, the capability of correlating the use of different thermal pretreatments and/or Pd metal loadings with the attainment of a high, controlled metal dispersion has been our primary goal.

Hydrogen chemisorption has been selected as the usual technique for measuring the metal dispersion, or the fraction of total metal atoms exposed (FE), specially in the case of supported noble metals. However, because hydrogen is also capable of absorbing in Pd to give palladium hydrides, refinements of the conventional chemisorption techniques were required to deal with the problem.

So, relevant, previous work on hydrogen solubility in Pd and on the formation of Pd-hydrides on supported particles of this metal again caught the attention of researchers in the field during the past decade, in an attempt to correlate the said features with the catalytic performance of this noble metal. In fact, Aben had already reported in the 1960s that the smaller particles of finely divided Pd (particle diameter ~25 Å) supported on SiO_2 adsorbed less hydrogen in the β-hydride phase than the larger particles of palladium black (particle diameter >500 Å) (*11*). Later, Boudart and Hwang studied the solubility of hydrogen in supported Pd for a broad range of FE and attempted to quantify it (*12*).

The use of contemporary, direct observation techniques, different from the volumetric methods, has begun to give more precise answers about the solubility of hydrogen in Pd crystallites in the range of 15–60 Å (*13–16*). At least three types of hydrogen associated to Pd have been discerned at typical H_2 chemisorption experimental conditions aimed at FE measurements: (i) chemisorbed, (ii) subsurface (*13, 14*) or "weakly chemisorbed" (*16*), and (iii) dissolved, forming the β-hydride phase, hydrogen (*13–16*).

Despite these precedents, the knowledge of the fraction of palladium hydride formed, as a function of the metal crystallite size in a supported Pd catalyst—under typical hydrogen chemisorption conditions—poses a more complex, still not completely clarified query. Hereby, then, we also focus our attention to the quantitative aspects of the superimposed hydrogen solubility phenomenon, using Benson *et al.*'s double isotherm H_2 chemisorption method (*17*) for measuring the FEs of the palladium crystallites of our Pd/SiO_2 preparations.

EXPERIMENTAL

Materials. Catalyst samples were obtained via ion exchange (IE) of $[Pd(NH_3)_4]^{2+}$, prepared from 99.5% w/w palladium acetate (Engelhard Corp.), on two commercial gels of silica (Davison G-59: S_g = 254 m^2/g, modal radius = 83 Å;

TABLE 1

Characteristics and Coding of the Catalyst Samples Used in This Work[a]

Silica support[b]	Palladium loading (% Pd w/w)	Pd surface coverage ($\theta = \Gamma_i/\Gamma_s$)[c]	Catalyst code sample
G-59	1.08	0.18	LG-59
	3.71	0.62	HG-59
G-03	2.16	0.20	LG-03
	7.71	0.72	HG-03

[a] After ion exchange (IE) of TPAcO in aqueous alkaline solution ($R = 30 \pm 0.5$ ml solution/g support; pH = 11 and $T = 297$ K), then washed at pH 11, and air dried at 298 K during 24 h in a forced convection oven.

[b] Davison types (W. R. Grace & Co.).

[c] Γ_i = mmol Pd/m^2, Γ_s = saturation value (*1*).

and Davison G-03: S_g = 558 m^2/g, modal radius = 16 Å).

Ion exchanges were made under standardized conditions, at pH = 11 and 298 K, in aqueous alkaline solution. After washing four times at pH = 11 with NH_4OH (aq.), the ion-exchanged samples were air dried at 298 K during 24 h in a forced convection stove. Support characterization and IE procedures have been fully detailed in previous work (*1*).

Palladium loadings were selected to obtain either low ($\theta \cong 0.2$) or high ($\theta \cong 0.6$–0.7) metal surface coverages (Table 1). Henceforth, the catalyst samples are coded either LG-*i* or HG-*i* for a straightforward follow-up.

Gas sources were: N_2 99.995% (Scott U.P.G.), H_2 99.999% (Scott U.P.G.), He 99.9999% (Matheson purity), and gas chromatography grade air. Hydrogen and nitrogen were prepurified with a 5-Å molecular sieve (Fisher Co.) and MnO/cellite cartridges. Air impurities were trapped with a tandem of a 5-Å molecular sieve and granulated ascarite (Riedel de Haën, pro-analysis) cartridges. Helium was used as purchased.

Apparatus. Calcination and reduction pretreatments, as well as hydrogen sorption measurements, were performed in a Pyrex microreactor loaded with approximately 150 μmol of Pd per catalyst sample. Its dead volume was reduced with Pyrex beads.

The microreactor was attached to a commercial sorptometer (Micromeritics, Accusorb 2100E), thus allowing the *in situ* attainment of successive experimental procedures on each protocol without exposing it to the atmosphere.

A PID temperature controller (PμP 2010) driving a cylindrical oven was used to calcine or reduce the materials, with a precision of ±1 K in the steady-state mode and ±0.1 K/min in the ramp mode.

The microreactor was submerged into a thermostatized water bath (Haake F3-C) during H_2 sorption experiments. Hydrogen uptakes were measured at 298.2 ± 0.5 K.

Calcining procedures. Different aliquots of the dried samples were calcined under nitrogen or air gas streams (200 ml STP/min) from ambient conditions to a predetermined final temperature (T_c) with a heating rate, β, of 6 K/min, then holding at T_c for 2 h, then cooling back to room temperature under gas flow.

Reducing procedures. Each of the calcined aliquots was first reduced under hydrogen flow (100 ml STP/min) right after the completion of the calcining procedure from ambient conditions to a predetermined final temperature (T_r), with β = 2 K/min. This final temperature was customarily held for 2 h, unless otherwise indicated.

Next, the hydrogen flow was stopped and the microreactor was evacuated to ca.

10^{-6} Torr (1 Torr $\equiv$ 133 N m^{-2}) at T_r, to initiate the elimination of all of the sorbed hydrogen. Then, the microreactor temperature was set at 653 K, while under vacuum. To this end, either the temperature was raised from T_r to 653 K, when $T_r < 653$ K (heating rate: 10 K/min) or the microreactor was cooled, when $T_r > 653$ K (cooling rate: 5 K/min). Finally, the samples were briskly cooled to room temperature, still *in vacuo,* prior to any of the H_2 uptake measurements.

Measurements of the exposed metal fraction (FE) and hydrogen solubility. The method of the hydrogen double isotherm, as described by Benson *et al.* (*17*), was employed to determine the FE as well as the solubility of hydrogen into the silica supported Pd crystallites, at 298.2 ± 0.5 K and 150 Torr of H_2.

First, the dead volume was determined with He (298.2 ± 0.5 K). Second, the system was evacuated during 60 minutes ($\cong 10^{-6}$ Torr) after which the first isotherm was measured, $P_{max.} = 200$ Torr. The system was again evacuated for 20 min down to $10^{-4} < P$ (Torr) $< 10^{-2}$ ($T = 298.2 \pm 0.5$ K) before measuring the second isotherm.

Hydrogen uptakes along both isotherms were measured by successively increasing the gas pressure, i.e., both are sorption isotherms. The pressure was let to stabilize prior to each registry; stabilization times ranged between 2 and 3 h per data point.

A further evacuation at RT ($P = 10^{-6}$ Torr; 20 min) followed by purging with He prior to the system opening (100 ml/min; 5 min) was found to be an adequate procedure to preserve the FE of the Pd crystallites upon any ulterior exposure of the catalysts to the atmosphere. Samples were kept into a dessicator for their later use in electron microscopy studies.

In what follows H_t indicates the total uptake of hydrogen at 150 Torr (atoms of sorbed hydrogen) from the first isotherm, whereas H_{ab} stands for the uptake of hydrogen at 150 Torr (atoms of absorbed hydrogen) from the second one. The difference between these two values is designated as H_{ad} (atoms of adsorbed hydrogen).

The exposed metal fraction (FE) was calculated by assuming the stoichiometry $H_{ad}/Pd_s = 1$ (*18–20*). Pd_s designates an atom of palladium of the crystallite surface. Therefore, FE equals H_{ad}/Pd_t hereafter.

Blank runs were made to verify the total absence of hydrogen sorption on the G-59 and G-03 supports in the pressure range used.

Transmission electron microscopy (TEM). Catalyst samples were finely crushed, dispersed in distilled water, and submerged in an ultrasonic bath for 5 min. A few drops of the sonicated suspensions were deposited onto 200-mesh copper grids furnished with a Formwar film and dried at RT for 30 min.

A JEOL 100CX electron microscope operating in the bright field mode with an accelerating voltage of 100 kV was employed to perform the TEM measurements.

Average volume-to-surface particle diameters ($\bar{d}_{TEM} = \sum n_i d_i^3 / \sum n_i d_i^2$) were obtained by counting about 100 particles, from 10 micrographs per sample, by considering the Pd crystallites spherical.

RESULTS

a. Exposed Metal Fraction of the Pd/SiO_2 Catalysts vs Pretreatment Conditions

a.1. Effect of calcining conditions. Table 2 shows the hydrogen uptakes and FE of the Pd/SiO_2 catalysts calcined at different maximum temperatures (T_c) under a stream of nitrogen or air, then reduced with hydrogen up to $T_r = 723$ K. Within the error bounds of the experimental method it can be observed that upon reduction for 2 h at that T_r, the FEs are the same for each of the catalysts, regardless of the calcination atmosphere.

Figure 1 shows the FE values vs the maximum (air) calcination temperature after reducing the catalyst samples at $T_r = 723$ K. It can be seen that: (i) for $T_c <$ 423 K the low-loading samples (LG-*i*) have lower FE the higher the maximum calcina-

TABLE 2

Hydrogen Uptakes and Exposed Metal Fraction (FE) of the Pd/SiO_2 Catalysts Reduced in H_2 (100 ml STP/min) up to T_r = 723 K (2 h) vs Calcining Conditions

Sample code	Calcining conditions[a]		Pd_t[b] (mol × 10^4)	$\frac{H_t}{Pd_t}$	$\frac{H_{ab}}{Pd_t}$	Exposed metal fraction (FE)[c]
	Gas	T_c (K)				
LG-59	N_2	643	1.561	1.04	0.28	0.76
	Air	298[d]	1.679	1.14	0.30	0.84
		423	1.562	1.08	0.29	0.78
		643	1.548	1.08	0.28	0.80
HG-59	N_2	643	1.963	0.82	0.26	0.56
	Air	298[d]	1.763[e]	0.86	0.46	0.40
		423	1.549	0.90	0.31	0.59
		643	1.745	0.84	0.27	0.57
LG-03	N_2	643	1.723	0.96	0.31	0.65
	Air	298[d]	1.722	1.07	0.31	0.76
		423	1.733	1.00	0.31	0.68
		643	1.740	0.92	0.30	0.62
HG-03	N_2	423	1.502	0.97	0.28	0.68
		453	1.820	0.85	0.26	0.59
		643	1.187	0.84	0.29	0.55
	Air	298[d]	1.442[e]	0.76	0.30	0.46
		423	1.311	0.91	0.28	0.63
		643	1.366	0.80	0.26	0.53
		723	1.254	0.73	0.25	0.48

[a] Gas flow rate = 200 ml STP/min; β = 6 K/min; 2 h at T_c.
[b] Total amount of Pd placed into the microreactor.
[c] FE = H_{ad}/Pd_t, $H_{ad} = H_t - H_{ab}$ (chemisorption stoichiometry: $H_{ab}/Pd_s = 1$).
[d] Sample was dried in a forced convection stove (24 h) at 298 K.
[e] Average value of two replicates.

tion temperature, whereas the high-loading ones (HG-*i*) show higher FE the higher the T_c; and (ii) for $T_c \geq 423$ K each of the supported Pd catalysts prepared with the macroporous SiO_2 (*i*G-59) have constant FE whatever the T_c, but those prepared with the microporous type (*i*G-03) have lower FEs when the maximum calcination temperature is increased.

Second, the low-loading preparations (LG-59 and LG-03) always give higher FEs than their respective high-loading counterparts (HG-59 and HG-03), as expected.

Finally, the FE values corresponding to LG-59 are always higher than those of LG-03, despite both catalysts having about the same Pd coverages ($\theta \cong 0.2$).

a.2. Effect of reducing conditions. Hydrogen uptakes and FE values vs maximum reduction temperature, T_r, of aliquots precalcined under different conditions are shown in Table 3. Quite significant decreases of FE result from the increase in T_r from 473 to 723 K in all of the catalyst samples previously calcined up to 643 K.

An apparent exception to this behavior was that of the LG-59 preparation upon its reduction at T_r = 473 K, which is presumably a consequence of the Pd being atomically dispersed on the G-59 silica and therefore incapable of chemisorbing hydrogen (*21*).

As exemplified in more detail for the HG-03 catalyst, the exposed metal fraction de-

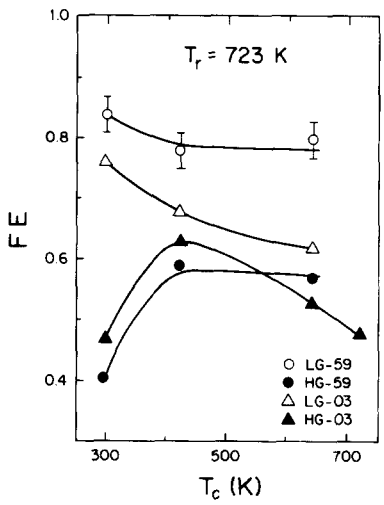

FIG. 1. Exposed metal fraction (FE) of Pd/SiO_2 catalyst samples with low (LG-*i*) and high (HG-*i*) metal loading on G-59 and G-03 Davison silicas vs the final calcining temperature in air (T_c), after H_2 reduction at 723 K (T_r). Calcining conditions: Air flow rate = 200 ml STP/min; β = 6 K/min; 2 h at T_c. Reducing conditions: H_2 flow rate = 100 ml STP/min; β = 2 K/min; 2 h at T_r.

creases markedly whenever $T_r > 673$ K independently of the calcining conditions, i.e., regardless of the T_c value or of the calcining atmosphere. No obvious FE vs T_r pattern is shown for $T_r < 673$ K.

The effect of reduction time on hydrogen uptakes and FEs was studied on a few aliquots of HG-*i* (Table 4). For both support types FE decreases the higher the reduction time, this decay being somewhat smaller on the microporous silica.

b. Variables Affecting the FE Measurements and the Pd Particle Size Estimates

Typical hydrogen sorption isotherms, corresponding to both high and low FE values are presented in Fig. 2. They show distinct features in each case, as a consequence of the different relative impact that the formation of palladium hydride has for each of them (*22*).

Figure 2a also shows that the system Pd–H_2 was properly equilibrated prior to the registry of equilibrium hydrogen pressures, since the experimental data points for the adsorption and desorption branches of the isotherms are coincidental. It is well documented that H_2 sorption/desorption isotherms on Pd only show hystheresis in the region of coexistence of the α- and β-hydrides on the phase diagram, but not where only one of these phases exists (*23*).

As already indicated in the Experimental section, hydrogen uptake registries were taken at 150 Torr and 298.2 ± 0.5 K. Additional experiments were conducted on an aliquot of HG-03 to analyze the effects of: (i) degasifying at the base pressure of $\cong 10^{-6}$ Torr and 653 K (2 h) and (ii) evacuating at different base pressures and for various lapses between both H_2 isotherms, on the hydrogen uptake and/or the calculated FE values.

Consistent values of H_2 uptakes and/or calculated FEs were obtained upon degasifying at 10^{-6} Torr and 653 K regardless of whether the dead volume was measured prior to the hydrogen sorptions or not. Besides, only the use of $10^{-4} < P$ (Torr) $< 10^{-2}$ of evacuation base pressure for 20–40 min between isotherms gave reproducible, consistent values of FE, whereas much lower values were obtained whenever the evacuation between isotherms was conducted at $\cong 10^{-6}$ Torr, thus indicating a loss of hydrogen chemisorbed on the Pd surface (*18*).

Benson *et al.* (*17*) established, on the other hand, that the evacuation at 0.01 kPa (~0.075 Torr) for 12 min at RT is sufficient for destroying the palladium β-hydride (with a very small fraction in the α-hydride form probably withstanding) but that the remaining hydrogen, chemisorbed on the surface of the metal crystallites, is not significantly removed. So, erroneous FE estimates are avoidable only by setting intermediate residual (i.e., base) pressures between H_2 sorption isotherms.

Using these consistent uptake measurements, the intrinsic error when estimating FE by means of the double isotherm method

TABLE 3

Hydrogen Uptakes and Exposed Metal Fraction (FE) of the Pd/SiO_2 Catalysts Calcined in N_2 and Air vs Maximum Hydrogen Reduction Temperature (T_r)

Sample code	Calcining conditions[a]		Maximum reduction temperature[b]	Pd_t[c] (mol × 10^4)	$\frac{H_t}{Pd_t}$	$\frac{H_{ab}}{Pd_t}$	Exposed metal fraction (FE)[d]
	Gas	T_c (K)	T_r (K)				
LG-59	N_2	643	473	1.574[e]	0.98	0.35	0.63
			723	1.561	1.04	0.28	0.76
HG-59	N_2	643	473	1.503	1.23	0.29	0.94
			723	1.963	0.82	0.26	0.56
LG-03	N_2	643	473	1.842	1.26	0.31	0.96
			723	1.723	0.96	0.31	0.65
HG-03	N_2	643	473	1.214	1.13	0.28	0.85
			573	1.395	1.04	0.27	0.77
			673	1.207	1.06	0.29	0.77
			723	1.187	0.84	0.29	0.55
	Air	298[f]	473	1.338	1.01	0.28	0.73
			673	1.392	1.03	0.30	0.73
			723	1.442[e]	0.76	0.30	0.46
		643	473	1.428	1.10	0.29	0.82
			723	1.366	0.80	0.26	0.53

[a] Gas flow rate = 200 ml STP/min; β = 6 K/min; 2 h at T_c.
[b] Hydrogen flow rate = 100 ml STP/min; β = 2 K/min; 2 h at T_r.
[c] Total amount of Pd placed into the microreactor.
[d] FE = H_{ad}/Pd_t, $H_{ad} = H_t - H_{ab}$ (Chemisorption stoichiometry: $H_{ab}/Pd_s = 1$).
[e] Average value of two replicates.
[f] Sample was dried in a forced convection stove (24 h) at 298 K.

TABLE 4

Hydrogen Uptakes and Exposed Metal Fraction (FE) of the High-Loaded Pd/SiO_2 Catalysts Dried in a Forced Convection Oven or Calcined in Air (200 ml STP/min) vs Hydrogen Reduction Time at 723 K

Sample code	Pd_t[a] (mol × 10^4)	Calcining conditions T_c (K)	Total reduction time at T_r (h)[b]	$\frac{H_t}{Pd_t}$	$\frac{H_{ab}}{Pd_t}$	Exposed metal fraction (FE)[c]
HG-59	1.593	298[d]	2	0.87	0.45	0.42
			8	0.80	0.41	0.39
			24	0.68	0.51	0.18
HG-03	1.254	723	2	0.73	0.25	0.48
			24	0.61	0.24	0.37

[a] Total amount of Pd placed into the microreactor.
[b] Hydrogen flow rate = 100 ml STP/min; β = 2 K/min, then holding at T_r.
[c] FE = H_{ad}/Pd_t, $H_{ad} = H_t - H_{ab}$ (Chemisorption stoichiometry: $H_{ab}/Pd_s = 1$).
[d] Sample was dried in a forced convection stove (24 h) at 298 K.

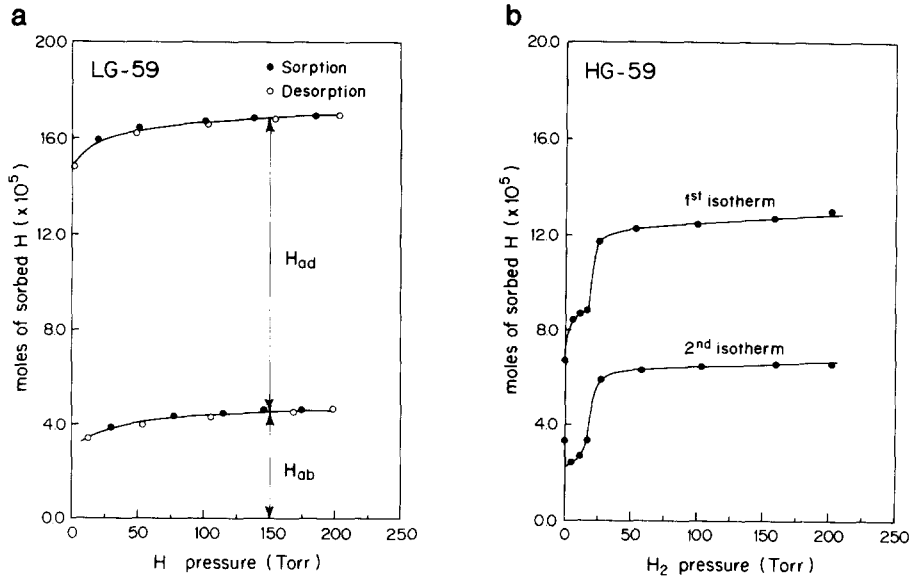

FIG. 2. Hydrogen sorption isotherm on Pd/SiO_2 measured at 298.2 ± 0.5 K for catalyst samples with: (a) High FE (0.80); corresponds to LG-59 (Pd_t = 1.55 × 10^{-4} mol) air calcined at T_c = 643 K, then H_2 reduced at T_r = 723 K for 2 h. (b) Low FE (0.39); corresponds to HG-59 (Pd_t = 1.59 × 10^{-4} mol) air dried at T_c = 298 K, then H_2 reduced at T_r = 723 K for 8 h.

was calculated to be within the ±0.03 confidence interval (FE units), for a 95% confidence level.

Palladium crystallite sizes assuming spherical particle shape were calculated from these H_2 chemisorption values, by means of the expression (*24*)

$$\bar{d}_q = \frac{11.2}{FE}, \qquad (1)$$

where $\bar{d}_q$ (Å) stands for the average or mean particle diameter.

These values are compared with those obtained by direct observation in the electron microscope ($\bar{d}_{TEM}$) in Table 5. There is a close agreement between both sets of values, although $\bar{d}_q$ was significantly higher than $\bar{d}_{TEM}$ for samples with larger crystallites pertaining to series which had been dried at 298 K and then H_2 reduced for a prolonged period. For this particle range, however, not only did the error propagation of the double-isotherm method become significant, but also some pore occlusion of the microporous silica by the Pd crystallites was made evident, as analyzed in the next section.

c. Hydrogen Solubility in Pd/SiO_2

Tables 2–4 condense the full set of hydrogen uptake measurements made during this experimental program. These values together with some obtained from additional runs are recast in Fig. 3, in which different variables are represented as a function of FE and/or $\bar{d} = \bar{d}_q \cong \bar{d}_{TEM}$.

As is fully discussed later, uptake data from certain runs were deliberately excluded when making Fig. 3. These data belong to samples that: (i) were exposed to prolonged reducing processes (longer than 2 h), or (ii) correspond to samples with $\bar{d}$ > 20 Å (FE < 0.56), for palladium supported on the microporous G-03, or (iii) had monoatomically dispersed Pd.

Figure 3a represents the total amount of sorbed hydrogen atoms per total amount of palladium atoms deposited onto the catalyst

TABLE 5

Average Diameter of the Palladium Crystallites of the Pd/SiO_2 Catalysts, Calculated from FE Values Estimated with H_2 Chemisorption Data ($\bar{d}_q$) vs TEM Measured Values ($\bar{d}_{TEM}$)

Sample code	Calcining conditions[a]		Reducing conditions[b] T_r (K)	$\bar{d}_q$[c] (Å)	$\bar{d}_{TEM}$[d] (Å)
	Gas	T_c (K)			
LG-59	N_2	643	723	15	15
HG-59	N_2	643	723	20	19
	Air	298[e]	723[f]	29	23
LG-03	Air	298[e]	723	15	14
HG-03	N_2	643	673	15	15
			723	20	20
	Air	298[e]	723[g]	30	25

[a] Gas flow rate = 200 ml STP/min; β = 6 K/min; 2 h at T_c.

[b] H_2 flow rate = 100 ml STP/min; β = 2 K/min; 2 h at T_r.

[c] Calculated from Eq. (1) ($\bar{d}_q \simeq 11.2/FE$).

[d] Volume-to-area average diameter = $\Sigma n_i d_i^3 / \Sigma n_i d_i^2$.

[e] Sample was dried in a forced convection stove (24 h) at 298 K.

[f] Sample was reduced for 8 h at the mentioned T_r.

[g] Sample was reduced for 24 h at the mentioned T_r.

(H_t/Pd_t) vs FE. This ratio increases markedly for high FEs, almost doubling that of the β-hydride phase of Pd black. The latter ratio, which was obtained in an additional experiment, coincides with that of previously reported data (*25*).

A full line illustrates the said upward trend, which agrees well with the (downward) behavior of the ratio of absorbed hydrogen atoms per total amount of palladium atoms (H_{ab}/Pd_t) vs FE, shown in Fig. 3b. This figure makes apparent that hydrogen solubility decreases the lower the Pd crystallite sizes, reaching a minimum (constant) value when $\bar{d} \leq 20$ Å, regardless of the level of Pd loading and/or the type of support silica onto which the metal was deposited.

The last figure in this series, Fig. 3c, shows the evolution of the ratio of absorbed hydrogen atoms to bulk palladium atoms (H_{ab}/Pd_b) vs FE. Bulk palladium stands for the substraction of surface palladium atoms from the total, $Pd_b = Pd_t - Pd_s$, assuming the stoichiometric ratio $H_{ad}/Pd_s = 1$.

The H_{ab}/Pd_b ratio becomes surprisingly large when $\bar{d} \leq 20$ Å. This striking feature led us to consider with further detail the chemisorption, solubility, and hydride formation capabilities of hydrogen on palladium, as enlightened from contemporary surface science studies (*19, 26–37*). The forthcoming hypotheses is discussed in the final section of the paper.

First H_{ab} was split into two terms,

$$H_{ab} = H_{ss} + H_\beta, \tag{2}$$

where

H_{ss}: Hydrogen atoms sorbed in subsurface sites, located between the first (surface) and the second layers of the Pd crystallite (*26–36*).

H_β: Hydrogen atoms absorbed below the second layer of Pd atoms of the crystallite, forming the β-hydride phase.

From Eq. (2) the following relationship is readily obtained:

$$\frac{H_{ss}}{Pd_s} = \frac{H_{ab}}{Pd_s} - \frac{(1 - FE)}{FE}\frac{H_\beta}{Pd_b}. \tag{3}$$

Hypothesizing that the ratio H_β/Pd_b falls linearly from 0.67, its value for bulk palladium (FE = 0) (*25*) to zero for monoatomic dispersion (FE = 1), obviously excluding this point, then

$$\frac{H_\beta}{Pd_b} = 0.67\,(1 - FE), \tag{4}$$

which is equivalent to writing

$$\frac{H_\beta}{Pd_t} = 0.67\,(1 - FE)^2. \tag{5}$$

From Eqs. (3) and (4) the following expression is finally obtained:

$$\frac{H_{ss}}{Pd_s} = \frac{H_{ab}}{Pd_s} - 0.67\frac{(1 - FE)^2}{FE}. \tag{6}$$

Using this last expression the ratios $H_{ss}/$

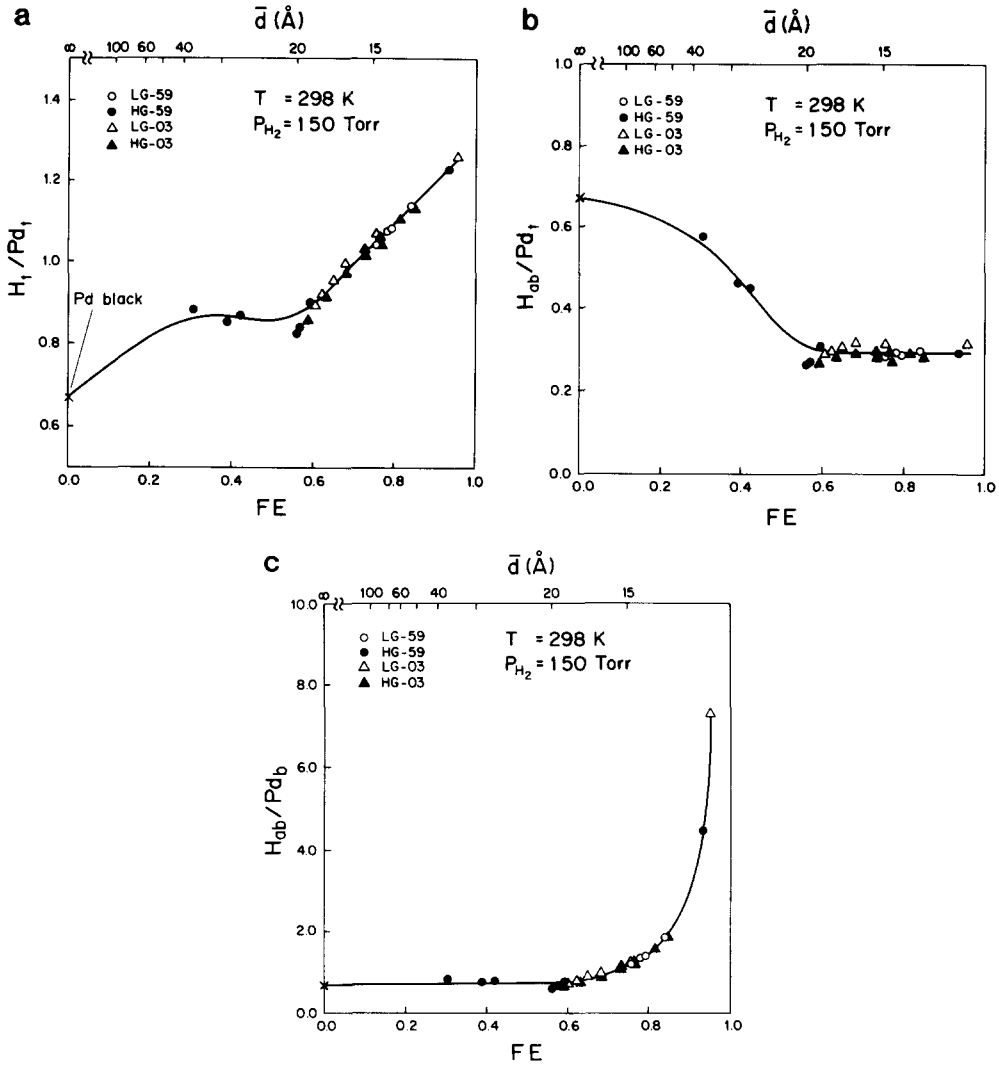

FIG. 3. Hydrogen uptakes, ratioed with the total (Pd_t) or bulk (Pd_b) amount of palladium in the system vs the exposed metal fraction and/or mean crystallite diameter ($\bar{d}$, from Eq. (1)) of Pd/SiO_2, calculated from H_2 chemisorption data taken from selected runs: (a) H_t/Pd_t; (b) H_{ab}/Pd_t; (c) H_{ab}/Pd_b (H_t = total H_2; H_{ab} = absorbed H_2; $H_{ad} = H_t - H_{ab}$). Full lines are merely indicative of functional "trends" (see text).

Pd_s vs FE and/or $\bar{d}$ were calculated for each of the different catalyst samples shown in Fig. 3 and are presented in Fig. 4. The latter figure shows that the H_{ss}/Pd_s ratio decays from ~1 for $\bar{d} = \infty$ (FE = 0) down to a constant value of about 0.3 for $\bar{d} \leq 20$ Å.

To verify whether the solubility traits presented in Figs. 3b and 4 had been observed by other workers who had used Benson *et al.*'s method, albeit employing alumina and titania besides SiO_2 as supporting materials, we referred to recent papers on the subject (*22, 38*) (Fig. 5). Excluded data points were those belonging to the following catalysts: (i) Pd/TiO_2 reduced at $T_r > 573$ K; (ii) Pd/Al_2O_3 reduced at $T_r \geq 773$ K; (iii) $Pd/(SiO_2–Al_2O_3)$ of very

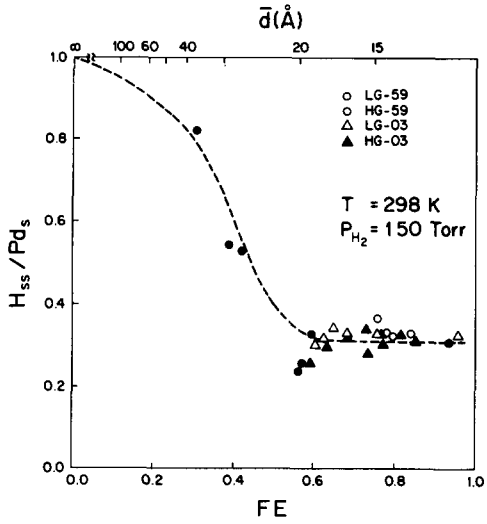

FIG. 4. Ratio of subsurface hydrogen to surface palladium, H_{ss}/Pd_s vs the exposed metal fraction and/or mean crystallite diameter ($\bar{d}$, from Eq. (1)) of Pd/SiO_2, calculated from H_2 chemisorption data taken from selected runs. The dashed line is merely indicative of a functional trend.

high surface areas, $S_g > 400$ m^2/g; and (iv) samples where $\bar{d}_q$ was larger than the medium radius of the support pores. Figure 5 shows that the combined results match fairly well.

Finally, Fig. 6 shows the ratio of H_{ab}/Pd_t vs FE corresponding to experimental data taken from: (i) any of our Pd/SiO_2 catalysts which were exposed to prolonged reducing processes (longer than 2 h), or correspond to Pd/G-03 samples with $\bar{d} >$ 20 Å; and (ii) the remaining Pd/TiO_2 and Pd/Al_2O_3 catalyst samples of Chou and Vannice (*22*) and Baker *et al.* (*38*) which were excluded when making Fig. 5, as well as Sudhakar and Vannice's results (*39*) for Pd/REO catalysts reduced at 573 K (REO: rare earth oxides).

It is apparent the suppression of hydrogen solubility, as expressed by the ratio H_{ab}/Pd_t, in those systems where decoration and encapsulation of Pd from the support occurs (Pd/TiO_2 and Pd/REO), those with very high support surface area (Pd/SiO_2–Al_2O_3 (*22*)), and the ones where $\bar{d}_q$ is larger than the medium radius of the support pores. Clearly, several of our Pd/SiO_2 catalyst preparations and/or their pretreatment histories cause them to lie within these bounds, especially since the IE was made at pH = 11 (*1*).

The dashed line in Fig. 6 corresponds to Eq. (5), from which it is straightforward to infer that all of the experimental data points located below it may represent severe cases of physical blockade of the Pd crystallites that may grossly distort their size estimates, as discussed below.

DISCUSSION

Effects of Calcining and Reducing Conditions and Support Structure on the FE of the Pd/SiO_2 Catalysts

As already indicated in the Introduction section of this paper, it was shown in previous work (*2*) that the resulting surface products from the IE of tetramminepalladium complex on Davison silicas (formally $[Pd(NH_3)_4]^{2+}[(SiO)]_2^{2-}$, and hereafter TPSiO) upon drying–calcination procedures can be strongly dependent on the pretreatment atmosphere and/or the support structure. Table 6 summarizes those results to help in the following discussion about the final fraction of total metal atoms exposed, FE.

The FE values vs the maximum (air) calcination temperature, T_c, after reducing the catalyst samples at T_r = 723 K indicated the presence of two well-differentiated regions below and above T_c = 423 K (Fig. 1).

Water-solvated amminepalladium complexes with more than two NH_3 ligands ($[Pd(NH_3)_n(H_2O)_{4-n}]^{2+}[SiO)_2]^{2-}$, $2 < n \leq 4$) are left on the supports upon calcining below T_c = 423 K. It is only when T_c = 423 K and the calcining gases are dried that the calcination product is the diamminepalladium complex (DPSiO) (*2*).

It is then only logical to think that if the solvated TPSiO and the intermediate complexes ($2 < n < 4$) had less interaction with the support surface, i.e., more mobility, the surface migration of these precursors of the

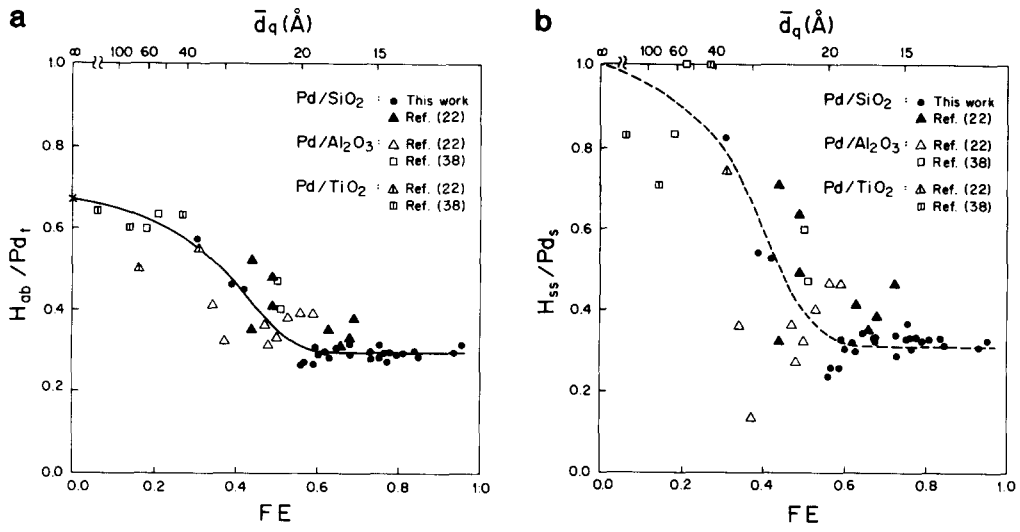

FIG. 5. Comparative values of the ratios of: (a) absorbed hydrogen to total supported palladium (H_{ab}/Pd_t) and (b) subsurface hydrogen to surface palladium (H_{ss}/Pd_s) vs the exposed metal fraction and/or mean crystallite diameter ($\bar{d}_q$, from Eq. (1)) on different supported Pd catalysts. Full and dashed lines are indicative of functional trends.

palladium crystallites would be hampered the higher than T_c, because the loss of NH_3 and H_2O solvation ligands leads stepwise to DPSiO, which is (claimed to be) more firmly anchored to the silica surfaces (*2*).

That was also the argumental line of Homeyer and Sachtler while interpreting their experimental results with $[Pd(NH_3)_4]^{2+}$ supported in NaY zeolite (*9*), and indeed the higher the T_c the higher the FE for the HG-*i* series of our catalysts in this low-temperature calcining region ($T_c < 423$ K).

Nevertheless, just the opposite occurred whenever catalyst preparations with low Pd coverages were dealth with, i.e., with the LG-*i* series. The calcining process implied the progressive heating of aliquots of the dried samples from ambient conditions to a predetermined final temperature, T_c, with a heating rate $\beta = 6$ K/min, then holding at the said T_c for 2 h. In our opinion, if the surface mobilities of the anchored ammine palladium complexes $[Pd(NH_3)_n(H_2O)_{4-n}]^{2+}$ ($2 \leq n \leq 4$) were not too different, mild calcining temperatures would not be high enough to allow for the coalescence, via sur-

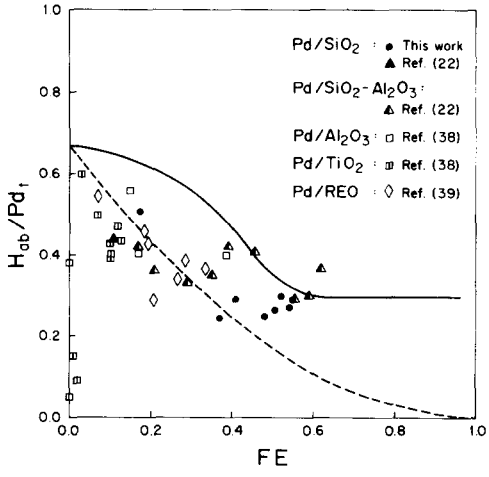

FIG. 6. Comparative values of the ratio of absorbed hydrogen to total supported palladium, H_{ab}/Pd_t, vs the exposed metal fraction and/or mean crystallite diameter ($\bar{d}_q$, from Eq. (1)) on different supported Pd catalysts where decoration, encapsulation, and/or occlusion has been reported. The full line is indicative of the functional trend proper of "unhindered" catalytic systems (see Fig. 5). The dashed line represents a normalized β-HPd vs FE relationship (see Eq. (5)).

TABLE 6

Resulting Pd Surface Species onto the Surfaces of Davison G-59 and G-03 Silica-Gels, from TPAcO Ion-Exchanged at pH 11 (297 K) vs Drying-Calcining Conditions (*2*)

Support type	Calcining conditions		Pd surface species onto the supports
	Atmosphere	T_c (K)	
G-59	N_2	423	$[Pd(NH_3)_2]^{2+}$
		643	Pd^0
	Air	298	$[Pd(NH_3)_4]^{2+}$
		423	$[Pd(NH_3)_2]^{2+}$
		643	Pd^{2+}
G-03	N_2	423	$[Pd(NH_3)_2]^{2+}$
		643	Pd^0
	Air	298	$[Pd(NH_3)_4]^{2+}$
		423	$[Pd(NH_3)_2]^{2+}$
		643	Pd^{2+} y Pd^0

face diffusion, of the more separated ($\theta \cong 0.2$) complexes of the LG-*i* catalysts throughout the calcining process, which certainly could—and seems to—happen with the sustained heating at higher T_c.

These increases in FE of the supported palladium at higher calcining temperatures for the HG-*i* preparations vs the observed *decreases* of FEs in the LG-*i* counterparts at correspondingly higher T_c would then imply a net predominance of the rate of nucleation rather than the rate of growth via coalescence in the high-loading series, with a conversely opposite pattern for the more isolated nuclei of the low-loading series.

Now, at higher calcining temperatures ($T_c \geq 423$ K) the FE of the Pd crystallites supported onto either silica were about the same regardless of the type of precursor(s) present onto the surfaces prior to initiating their reduction with hydrogen, that is, regardless of the calcining gas (N_2 or air) previously employed (see Tables 2 and 6). This behavior was common to both the high-loaded (HG-*i*) or the low-loaded (LG-*i*) systems.

However, at these higher T_c only the FEs of Pd supported onto G-59 remained about constant for both the HG-59 and the LG-59 samples whatever the T_c. That is, the final size of the palladium crystallites is solely a function of the metal loading on the macroporous support. Conversely, the higher the T_c the lower the FE on the microporous G-03, for both the HG-03 and the LG-03 samples.

Being that these silicas are chemically equivalent (*1*), only their structural differences (modal radii = 83 and 16 Å for G-59 resp. G-03) are to be primarily scrutinized to account for these dissimilar behavioral patterns. So, a microporous structure such as that of G-03 might favor the growth of metal particles, probably via coalescence of precursor metal clusters opposite to each other into the pore walls.

This might be also the cause of the consistently lower FE values on G-03 resp. G-59 beyond $T_c = 600$ K.

A seemingly alternate explanation saying that due to diffusional constraints the water molecules produced during the calcining process in air would be able to attach as solvating ligands to neighboring diammine complexes rather than to primarily diffuse outward inside the narrow pores of G-03 (thus favoring a competitive coalescing or surface diffusional pathway) has to be discarded: were that the case, certainly the FEs after nitrogen calcining would have been higher than those after air calcining at corresponding T_c's (See Table 2).

With regard to the influence of the reducing conditions on the FE of our Pd/SiO_2 catalysts, it can be concluded that when the deammination of the TPSiO is complete upon calcining ($T_c \geq 643$ K), the ratio of nucleation vs crystal growth rates decreases the higher the T_r.

Finally, it was shown that the reduction times in hydrogen ($T_r = 723$ K) are more deletereous for obtaining high Pd metal dispersions on a macroporous silica (G-59) than on a microporous type (G-03). This feature exposes that under certain circumstances the use of a microporous support can help in controlling the final crystallite size. The

topic is further analyzed below, together with the discussion about the "suppression" of hydrogen absorption. In passing, said feature has been also reported for the Pd/NaY system (*8, 40*).

Hydrogen Solubility in Pd Crystallites Supported in SiO_2

The concept of hydrogen solubility in supported palladium particles has been interpreted in different ways by workers in the field. The ratios H_t/Pd_t, H_{ab}/Pd_t, or H_{ab}/Pd_b have been indistinctly used, presumably in conformity with their proximity to the stoichiometric value of the β-hydride phase (in the metal dispersion range used).

Although at first sight there is no "apparent" reason for choosing a specific ratio, we consider H_{ab}/Pd_t to be the most suitable one for a quantitative follow-up of hydrogen solubility because:

(i) H_t/Pd_t includes a portion of hydrogen which is chemisorbed onto the crystallites (and which becomes increasingly important the higher the metal dispersion), whereas the concept of solubility in continua obviously calls upon bulk properties, and

(ii) H_{ab}/Pd_b induces into thinking that part of the "solvent" (Pd_s) does not intervene in the solubilization process.

Thus, the ratio H_{ab}/Pd_t conceptually appears as most adequate, albeit it is certainly not exempt from inconsistencies of its own: H_{ab} is related to H_{ad} through H_{ss} (see Eq. (2)), but the latter can be considered an intermediate of hydrogen solubilization in bulk Pd (*27, 41*).

Having justified the choice of the ratio H_{ab}/Pd_t as the most suitable for quantifying hydrogen solubility in crystallites of supported Pd, we now discuss our experimental data. In the Results section it was pointed out that the ratios H_t/Pd_t, H_{ab}/Pd_t, and H_{ab}/Pd_b for Pd/SiO_2 strongly correlate with FE and/or $\bar{d}$ whenever geometric constraints and/or encapsulation artifacts are absent. It was also shown that hydrogen solubility, as expressed by H_{ab}/Pd_t, decreases the higher the FE until it reaches a constant plateau of about 0.3, for FEs larger than 0.6 (i.e., for particle diameters smaller than ~20 Å).

On the contrary, Boudart and Hwang (*12*) reported that the hydrogen solubility, as expressed by a parameter m' entirely equivalent to H_{ab}/Pd_t, decreased steadily the higher the FE, which contradicts our experimental results.

It is likely that the reasons for this discrepancy may behoove entirely on procedural matters, among which two possible candidates are:

(i) The evacuation conditions prior to the measurement of the second hydrogen isotherm. Boudart and Hwang did not specify theirs.

(ii) The method for calculating FE. Said authors used H_2–O_2 titrations as a way of getting independent figures of Pd_s, not tainted with the solubility values, even for samples with FE = 0.73. More recently it has been shown, though, that the stoichiometry of O_2 adsorption on Pd supported on various supports is a strong function of the metal crystallites particle size (*42*).

We resorted, instead, to TEM measurements as a check-up technique, in addition to rigorously controlled evacuation conditions and the analysis of a large number of replicates. Figure 5 shows a satisfactory agreement between this work and recent results presented by Chou and Vannice (*22*) and Baker *et al.* (*38*) (a certain degree of scatter among data points is to be attributed to somewhat different measuring conditions). These authors obtained independent FE data either from chemisorption of gases other than hydrogen (*22*) or TEM (*38*).

A second issue worth mentioning relates to the controverted assignment of H_{ss} as "subsurface hydrogen" onto each of the crystal faces of palladium, upon exposing the metal to hydrogen. Theoretical work by Muscat (*19*) reports on the existence of a special type of "weakly chemisorbed hydrogen" onto Pd(100), with strongly sorbed hydrogen being located between the first and

the second Pd layers, inward from the surface. But Rieder and Stocker (*37*) contradict Muscat's opinion, pointing out that the excess of hydrogen that can chemisorb onto Pd(100) locates in subsurface sites.

For the (111) and (110) faces of Pd single crystals, the concept of subsurface hydrogen enjoys a sizable amount of consensus (*26–36*), as it does for bulk polycrystalline Pd (*41, 43–46*) or supported Pd crystallites (*13, 14, 47*). Yet, some other authors talk about "weakly chemisorbed hydrogen" when describing measurements made under equal experimental conditions (*16, 41*), probably because in both cases the calculated hydrogen (ad)sorption energies are smaller than that of chemisorbed hydrogen but larger than the one for bulk dissolved H_2 forming the β-hydride phase (*48*). For our present purposes, though, what matters is that H_{ab} has to be split into two terms: H_{ss} and H_β.

Now, we have besides hypothesized that the ratio H_β/Pd_b decays—linearly—the larger the FE. The need for such an hypothesis is sustained on three facts:

—First, Renouprez and co-workers have observed that on Pd crystallites of about 15 Å or smaller, palladium hydride forms with a stoichiometric ratio lower than that on bulk palladium (*13, 14*).

—Second, at high dispersions supported Pd clusters rather than ordinary metal crystallites are formed. These have been assumed to be cuboctahedral by some workers (*14, 15, 49*), but there is wide consensus that the most stable shape for small metal clusters of metal with fcc crystal structure is icosahedral (*51, 51*).

Whichever the crystal shape be, though, the smallest cluster for which *both* surface and bulk atoms can be distinguished has a minimum of 13 atoms ($N = 13$), 12 of which are surface ones (See Fig. 7). Under this extreme situation the existence of H_β can no longer be envisioned, as the classical bulk octahedral sites for the formation of the β-hydride are entirely absent. In other words,

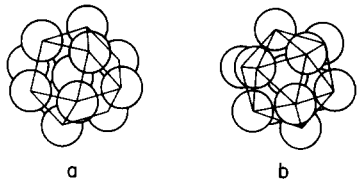

FIG. 7. Most stable shapes of smallest fcc metal crystallites: (a) cuboctahedron (*51*) and (b) Mackay's icosahedron (*52*). Each cluster has a total of 13 atoms, 12 of which are surface atoms ($N = 13$, $N_s = 12$; FE = 12/13 = 0.92).

there is a tangible limit for which $H_\beta/Pd_b = 0$. These clusters with $N = 13$ imply an FE = 12/13 = 0.92, and a particle diameter of about 7 Å for the cube-octahedron (*53, 54*).

—Finally, the availability of theoretical calculations indicating the number of bulk octahedral sites in clusters of various sizes and/or shapes is lacking. As H_β localizes in those sites, only from such a kind of data a more sound functional relationship for H_β/Pd_b vs FE other than a linear decay could be put forward.

Thus, for the time being, Eq. (4) appears as the simplest option able to retain the needed physico-chemical insight on the matter.

We are now in a position to retake the experimental data for further analysis. For instance, the surprising growth of H_{ab}/Pd_b the higher the FE (Fig. 3c) as due to the increased value of the ratio Pd_s/Pd_b together with the (associated) decrease of H_{ss}/Pd_s.

As has already been indicated, there is growing evidence about hydrogen locating in subsurface sites during adsorption/desorption cycles on Pd and other Group VIII metals, but quantitative estimates about the H_{ss}/Pd_s stoichiometry are scarce. According to Rieder *et al.* (*28*) the said ratio equals one and, according to this, H_{ss} would occupy every octahedral site between the first and the second surface layers of bulk Pd. Leary *et al.* (*47*) also used a one-to-one stoichiometry to interpret and model deuterium TPD spectra of Pd/SiO_2 (FE = 0.09–0.15) satisfactorily.

Figures 4 and 5a show a fairly good agreement with Rieder's finding in the limit of low Pd dispersion on several supports. Besides, this indicates that the evacuation conditions used in this work are adequate for removing both H_β and H_{ss}.

On the other hand, the experimental values for the ratio H_{ss}/Pd_s decrease steadily the lower the Pd particle size, until they reach a minimum asymptotic value of ~0.3 for FE $\geq$ 0.60 ($d \leq 20$ Å).

So far, despite voluminous work of hydrogen sorption on metals, few work has been devoted to rationalize the quantification of H_{ss} on supported metal catalysts. Thus, Vannice's group (*16, 22, 39*) only reported solubility values defined from the ratio H_{ab}/Pd_b, without further elaboration; likewise, Baker *et al.* (*38*) focused their work on SMSI effects. Goodwin and co-workers, however, have shown that the fraction of hydrogen which is reversibly chemisorbed (that is, weakly chemisorbed) on highly dispersed Ru on NaY zeolites is a function of the mean particle diameter (*55*). They were able to demonstrate that, in equilibrium, this hydrogen can accomodate on multiatomic sites similar to the B_5 ones described by van Hardeveld and Hartog (*53*).

Summing up, since both geometrical and electronic properties vary markedly for small metal crystallites (*56*), the asymptotic minimum of the H_{ss}/Pd_s for particles with $\overline{d} \geq 20$ Å (Fig. 4) has no obvious explanation to us, at least on the basis of the results from this work.

As for the suppression of hydrogen solubility in Pd crystallites deposited onto oxide supports, it is necessary to point out that although the calculation of FE via H_2 chemisorption data may yield good estimates of metal dispersion, this does not necessarily lead to equally good estimates of the mean metal particle size (*38, 57*).

For instance, Baker *et al.* reported that for Pd/TiO_2 catalysts reduced at 623 K hydrogen chemisorption data gave accurate values for the FE, but the mean particle diameter calculated from them ($\overline{d}_q$ = 120 Å) was notoriously far off the TEM value ($\overline{d}_{TEM}$ = 40 Å) (*38*).

This example clearly shows that whenever decoration, encapsulation, and/or occlusion of the Pd crystallites from promoters or supports is suspected, it will be neccesary to relate H_{ab}/Pd_t with $\overline{d}_{TEM}$, since $\overline{d}_q$ will no longer be a good estimator for the mean particle size of the metal crystallites. So, taking again the Pd/TiO_2 as an example, let us compare the value of H_{ab}/Pd_t measured by Baker *et al.*, ~0.40 (*38*), with the *expected* value for this ratio obtained from their $\overline{d}_{TEM}$ (40 Å), by entering Fig. 3b from above and then leftwards (after intersecting the "normal" trend for unoccluded crystallites): H_{ab}/Pd_t should have been 0.57 instead.

Similarly, for our HG-03 samples reduced 24 h at 723 K the measured value of H_{ab}/Pd_t was 0.24 (See Table 4), whilst $\overline{d}_{TEM}$ was 25 Å. From this measured diameter, Fig. 3b indicates that if it were not for the presence of obvious "geometric constrictions" H_{ab}/Pd_t should have been 0.40 instead.

Consequently, physical/structural occlusion of the Pd crystallites from both reducible or irreducible supports seems to produce a real suppression of hydrogen solubility at 373 K within the typical time scale of these chemisorptive methods.

This may be due to a variety of causes. On one hand, the suppression of H_{ss} in those regions where the support—or promoter—covers the Pd_s is likely and, on the other hand, it is also likely the suppression or diminishing of H_β in occluded or encapsulated crystallites, since the formation of the β-HPd phase is accompanied by an expansion of the crystal lattice, be it supported (*14, 15*) or bulk Pd metal (*58*). Naturally, severe thermal treatments may also lead to alloying of the palladium with the support (*38, 59*).

CONCLUSIONS

It is feasible to obtain of Pd/SiO_2 catalysts with a broad range of metallic dispersion or total exposed metal fraction (FE =

0.20–0.98) by controlling the Pd loading and the calcining and reducing conditions, using halide-free $[Pd(NH_3)_4]^{2+}/SiO_2$ precursors.

A critical value for the calcining temperature was found, 423 K, below which the final FE depends upon both the Pd loading and the type of amminepalladium complex onto the silica surfaces. Above T_c = 423 K the final FE is then a function of the Pd loading and the support structure, but indifferent to the type of precursor palladium species, contrarily to the reported behavior when zeolite supports are employed.

The application of a slightly modified version of Benson *et al.*'s (*17*) double-isotherm method, with strictly controlled parameters for temperature and degree of vacuum used, gives satisfactory, consistent H_2 uptake values in each of the Pd/SiO_2 systems. The calculated FE of the supported metal gives, in turn, direct estimates of the mean diameter sizes of the Pd crystallites, which are in good agreement with those measured by using TEM if and when their diameter is smaller than the modal radius of the support.

Bearing in mind the latter restrictions, the solubility of hydrogen on the supported Pd crystallites was quantified for most of the FE range, using the H_{ab}/Pd_t ratio as the solubility criterion. These calculated values correlate well with previously reported work where some other supports besides silica were used.

A monotonic, decreasing dependence between the amount of subsurface hydrogen and Pd crystallite diameter was found, but a rationale for it could not be discerned. It is felt that further research on the matter may be of help for a further understanding of hydrogenation reactions with Pd.

Using the above mentioned H_{ab}/Pd_t solubility criterion vs FE it was also verified for these Pd/SiO_2 systems (i.e., for catalysts where metal support interactions are minimal) that the occlusion (or self-occlusion) of Pd in the support micropores may lead to severe suppression of the phenomenological "hydrogen solubility."

In this regard, the generalized use of the functional relationship between H_{ab}/Pd_t vs FE (as depicted in Fig. 3b) is put forward as a valid criterion for estimating Pd crystallite sizes, since a departure from the usual "trend" acts as an automatic warning about decoration, encapsulation, and/or occlusion problems which will demand further characterization work.

ACKNOWLEDGMENTS

Thanks are given to José L. Giombi and María J. Yáñez for technical assistance, and to Professor Cristina E. González for her help in revising the English version of the manuscript. DAREX S.A.I.C. kindly provided the Davison silica gels. We acknowledge the financial aid received from the National Council for Scientific and Technical Research of Argentina (CONICET) and from the Universidad Nacional del Litoral (Santa Fe, Argentina).

REFERENCES

1. Bonivardi, A. L., and Baltanás, M. A., *J. Catal.* **125,** 243 (1990).
2. Bonivardi, A. L., and Baltanás, M. A., *Thermochim. Acta* **191,** 63 (1991).
3. Dalla Betta, R. A., and Boudart, M., *in* "Proceedings, 5th International Congress on Catalysis, Palm Beach, 1972" (J. W. Hightower, Ed.), p. 1329. North-Holland, Amsterdam, 1973.
4. Reagan, W. J., Chester, A. W., and Kerr, G. T., *J. Catal.* **69,** 89 (1981).
5. Park, S. H., Tzou, M. S., and Sachtler, W. M. H., *Appl. Catal.* **24,** 85 (1986).
6. Tzou, M. S., Jiang, H. J., and Sachtler, W. M. H., *React. Kinet. Catal. Lett.* **35,** 207 (1987).
7. Tzou, M. S., Jiang, H. J., and Sachtler, W. M. H., *J. Catal.* **113,** 220 (1988).
8. Bergeret, G., Gallezot, P., and Imelik, B., *J. Phys. Chem.* **85,** 411 (1981).
9. Homeyer, S. T., and Sachtler, W. M. H., *J. Catal.* **117,** 91 (1989).
10. Homeyer, S. T., and Sachtler, W. M. H., *J. Catal.* **118,** 266 (1989).
11. Aben, P. C., *J. Catal.* **10,** 224 (1968).
12. Boudart, M., and Hwang, H. S., *J. Catal.* **39,** 444 (1975).
13. Jobic, H., and Renouprez, A., *J. Less-Common Met.* **129,** 311 (1987).
14. Moraweck, B., Clugnet, G., and Renouprez, A., *J. Chim. Phys.* **83,** 265 (1986).
15. Davis, R. J., Landry, S. M., Horsley, J. A., and Boudart, M., *Phys. Rev. B* **39,** 10580 (1989).
16. Chen, A. A., Benesi, A. J., and Vannice, M. A., *J. Catal.* **119,** 14 (1989).
17. Benson, J. E., Hwang, H. S., and Boudart, M., *J. Catal.* **30,** 146 (1973).

18. Conrad, H., Ertl, G., and Latta, E. E., *Surf. Sci.* **41,** 435 (1974).
19. Muscat, J.-P., *Surf. Sci.* **110,** 85 (1981).
20. Behm, R. J., Christmann, K., and Ertl, G., *Surf. Sci.* **99,** 320 (1980).
21. See, for example, Kubas G. J., *Acc. Chem. Res.* **21,** 120 (1988); Ozin, G. A., and García-Prieto, J., *J. Am. Chem. Soc.* **108,** 3099 (1986); Nakatsuji, H., Hada, M., and Yonezawa, T., *J. Am. Chem. Soc.* **109,** 1902 (1987); Nakatsuji, H., and Hada, M., *J. Am. Chem. Soc.* **107,** 8264 (1985).
22. Chou, P., and Vannice, M. A., *J. Catal.* **104,** 1 (1987).
23. Wicke, E., and Blaurock, J., *J. Less-Common Met.* **130,** 351 (1987).
24. Anderson, J. R., "Structure of Metallic Catalysts." Academic Press, London, 1975.
25. Scholten, J. J. S., and Konvalinka, J. A., *J. Catal.* **5,** 1 (1966).
26. Cattania, M. G., Penka, V., Behn, R. J., Christmann, K., and Ertl, G., *Surf. Sci.* **126,** 382 (1983).
27. Behm, R. J., Penka, V., Cattania, M. G., Christmann, K., and Ertl, G., *Surf Sci.* **78,** 7486 (1983).
28. Rieder, K. H., Baumberger, M., and Stocker, W., *Phys. Rev. Lett.* **51,** 1799 (1983).
29. Grenter, F., Eberhardt, W., Di Nardo, J., and Plummer, E. W., *J. Vac. Sci. Technol.* **18,** 433 (1981).
30. Eberhardt, W., Grenter, F., and Plummer, E. W., *Phys. Rev. Lett.* **46,** 1085 (1981).
31. Eberhardt, W., Louie, S. G., and Plummer, E. W., *Phys. Rev. B* **28,** 465 (1983).
32. Felter, T. E., and Sowa, E. C., *Phys. Rev. B* **40,** 891 (1989).
33. Chan, C. T., and Louie, S. G., *Phys. Rev. B* **30,** 4153 (1984).
34. Daw, M. S., and Baskes, M. I., *Phys. Rev. B* **29,** 6443 (1984).
35. Daw, M. S., and Foiles, S. M., *Phys. Rev. B* **35,** 2128 (1987).
36. Muscat, J.-P., *Surf. Sci.* **148,** 237 (1984).
37. Rieder, K. H., and Stocker, W., *Surf. Sci.* **148,** 139 (1984).
38. Baker, R. T. K., Prestridge, E. B., and McVicker, G. B., *J. Catal.* **89,** 422 (1984).
39. Sudhakar, C., and Vannice, M. A., *J. Catal.* **95,** 227 (1985).
40. Homeyer, S. T., Karpinski, Z., and Sachtler, W. M. H., *Recl. Trav. Chim. Pays-Bas* **109,** 81 (1990).
41. Lynch, J. F., and Flanagan, T. B., *J. Phys. Chem.* **77,** 7628 (1973).
42. Martín, M. A., Pajares, J. A., and González Tejuca, L., *Z. Phys. Chem.* **140,** 107 (1984); *Nouv. J. Chim.* **9,** 261 (1985); *React. Kinet. Catal. Lett.* **31,** 1 (1986).
43. Aldag, A. W., and Schmidt, L. D., *J. Catal.* **22,** 260 (1971).
44. Eley, D. D., and Pearson, E. J., *J. Chem. Soc. Faraday Trans 1* **74,** 223 (1978).
45. Kisinova, M., Bliznakov, G., and Surnev, L., *Surf. Sci.* **94,** 169 (1980).
46. Jobic, H., Candy, J.-P., Perrichon, V., and Renouprez, A., *J. Chem. Soc. Faraday Trans 1* **81,** 1955 (1985).
47. Leary, K. J., Michaels, J. N., and Stacy, A. M., *Langmuir* **4,** 1251 (1988).
48. Paál, Z., and Menon, P. G., *Catal. Rev.-Sci. Eng.* **25,** 229 (1983).
49. Avery, N. R., and Sanders, J. V., *J. Catal.* **18,** 129 (1970).
50. See, for example, Allpress, J. G., and Sanders, J. V., *Surf. Sci.* **7,** 1 (1967); Gillet, M., *Surf. Sci.* **67,** 139 (1977); Burton, J. J., *Catal. Rev.* **9,** 209 (1974).
51. Hoare, M. R., and Pal, P., *Adv. Phys.* **20,** 165 (1971).
52. Hoare, M. R., *in* "Advances in Chemical Physics" (I. Prigogine and S. A. Rice, Eds.), Vol. 40, p. 49. Wiley, New York, 1979.
53. Van Hardeveld, R., and Hartog, F., *Surf. Sci.* **15,** 189 (1969).
54. Weats, R. C., "Handbook of Chemistry and Physics," 67th ed. CRC Press, Boca Raton, FL, 1986.
55. Sayari, A., Wang, H. T., and Goodwin, J. G., Jr., *J. Catal.* **93,** 368 (1985); Chen, Y. W., Wang, H. T., and Goodwin, J. G., Jr., *J. Catal.* **83,** 415 (1983); Yang, C.-H., and Goodwin, J. G., Jr., *J. Catal.* **78,** 182 (1982); Goodwin, J. G., Jr., *J. Catal.* **68,** 227 (1981).
56. Che, M., and Bennett, C. O., *in* "Advances in Catalysis" (D. D. Eley, H. Pines, and P. B. Weisz, Eds.), Vol. 36, p. 55. Academic Press, New York, 1989.
57. Bond, G. C., *in* "Spillover of Adsorbed Species" (G. M. Pajonk, S. J. Teichner, and J. E. Germain, Eds.), Vol. 17, p. 1. Elsevier, Amsterdam, 1983.
58. Maeland, A. J., and Gibb, T. R. P., Jr., *J. Phys. Chem.* **65,** 1270 (1961).
59. Juszczky, W., and Karpinski, Z., *J. Catal.* **117,** 519 (1989); Kepinski, L., *React. Kinet. Catal. Lett.* **38,** 363 (1989); Schleich, D., Schmeisser, D., and Göpel, W., *Surf. Sci.* **191,** 367 (1987).